

**THIS BOOK
CONTAINS
NUMEROUS
PAGES WITH
THE ORIGINAL
PRINTING ON
THE PAGE BEING
CROOKED.**

**THIS IS THE
BEST IMAGE
AVAILABLE.**

THE EFFECTS OF IN-PLANE RADIAL LOADS
ON THE VIBRATION OF CIRCULAR
SAW BLADES

by 6791

RONALD R. LEATHERS
B.S., Kansas State University, 1969

A MASTER'S REPORT

submitted in partial fulfillment of the
requirements for the degree

MASTER OF SCIENCE

Department of Mechanical Engineering

KANSAS STATE UNIVERSITY
Manhattan, Kansas

1971

Approved by:

F. C. Appl
Major Professor

L D
2668
R 4
1971
L 35
C. 2

TABLE OF CONTENTS

Chapter	Page
NOMENCLATURE.	v
INTRODUCTION.	1
DESIGN.	3
EXPERIMENTAL TECHNIQUE.	7
RESULTS	10
CONCLUSIONS	30
BIBLIOGRAPHY.	31
APPENDIX.	32

LIST OF TABLES

Table	Page
I. Theoretical Load Frequency Data for the Clamped-Free Saw Blade.	33
II. Experimental Load Frequency Data for the First Resonant Condition.	33
III. Experimental Load Frequency Data for the Second Resonant Condition.	34
IV. Experimental Load Frequency Data for the Third, Fourth, and Sixth Resonant Conditions	34
V. Experimental Load Frequency Data for the Fifth Resonant Condition.	35
VI. Experimental Load Frequency Data for the Seventh Resonant Condition.	36

LIST OF FIGURES

Figure	Page
1. Saw Blade Showing Geometry, Loading, and Boundary Condition.	2
2-3. Photograph of the Testing Device.	4
4. Three View Full Size Loading Fixture.	5
5. Shaker and Velocity Probe Placement	8
6. Frequency versus Nodal Diameters for the Clamped-Free Boundary	13
7-10. Theoretical Frequency of a Clamped-Free Blade with Radial In-Plane Load	14-17
11. Frequency versus Load for the First Resonant Condition	18
12. Frequency versus Load for the Second Resonant Condition	19
13. Frequency versus Load for the Fifth Resonant Condition	20
14. Frequency versus Load for the Sixth Resonant Condition	21
15. Frequency versus Load for the Seventh Resonant Condition	22
16. Sand Pattern for Second Resonant Condition Mode Shape.	23
17-18. Sand Pattern Mode Shape for a Resonant Condition. . .	24
19-20. Sand Pattern Mode Shape for the Fourth Resonant Condition	25
21. Sand Pattern Mode Shape for the Fifth Resonant Condition	26
22. Sand Pattern Mode Shape for a Resonant Condition. . .	26
23-24. Sand Pattern Mode Shape for the Sixth Resonant Condition	27
25-28. Sand Pattern Mode Shape for the Seventh Resonant Condition.	28-29

NOMENCLATURE

D	plate rigidity = $Eh^3/12(1-\nu^2)$
D_a	diameter of central hole in blade
D_b	blade clamping diameter
D_e	blade diameter
E	modulus of elasticity
F	frequency of the vibrating blade
h	blade thickness
i	number of nodal circles
n	number of nodal diameters
P	magnitude of the in-plane load
P_{cr}	critical load for a clamped-free blade
R	outside radius of blade
R_a	radius of central hole in blade
R_b	blade clamping radius
ν	Poisson's ratio

INTRODUCTION

The stability and vibration of circular plates has been studied for over 150 years. Kirchhoff (5)* in 1850 showed that it was possible to describe the modes of vibration of circular uniform thickness plates in terms of nodal diameters and nodal circles. Bryan (1) in 1891 began stability investigations of circular plates. A treatise by Southwell (6) in 1922 considered the free transverse vibration of a thin rotating disk clamped at its center.

Many studies have taken into account stresses due to thermal gradients, tensioning, and transverse loadings. In a dissertation by St. Cyr (7) in 1965, the vibration and stability of a circular plate clamped at its center and subjected to a concentrated radial load was considered. Dubois (3) in 1970 was able to duplicate St. Cyr's (7) results using a digital computer. Also, Dubois (3) included cases of tensioning and noted that the program could be extended to include calculation of the vibration characteristics.

One problem encountered in rock sawing has been termed off-sawing. The saw blade becomes warped and is then unfit for further use. It has been observed that the radial in-plane load on the blade may be approaching the critical value. One favorable

*Numbers in parentheses designate entries in Selected Bibliography.

result of tensioning of saw blades has been an increase in the buckling load for the blade. This report was an experimental investigation of variations in the vibration characteristics caused by concentrated in-plane radial loads for a non-rotating saw blade without gullets. The uniform thickness circular saw blade blank was clamped at a given radius. The blank had no tensioning. However, there may have been some residual stresses resulting from the manufacturing process. The saw blade during operating conditions experiences transverse friction forces while in contact with the rock. This situation was simulated by a fixed boundary condition at the point of load application as shown in Fig. 1.

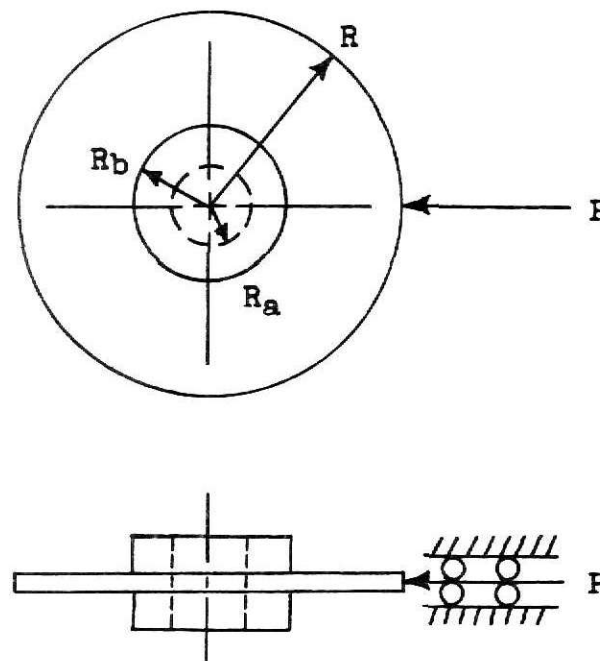


Figure 1

Saw blade showing geometry, loading, and boundary condition.

DESIGN

Preliminary design criteria:

1. The blade surface was to lie in a horizontal plane for observation of the mode shapes.
2. The base structure should contain a sufficient amount of weight to avoid fastening it to another structure.
3. The base structure should be wide enough to support an 8 inch cylindrical clamping fixture.
4. The base structure should be long enough to anchor a loading device which was to be 30 inches long.
5. The mass of the loading fixture was to remain at a minimum.
6. The blade, at the point of load application, was to have rotation and no translation in the vertical plane.
7. The maximum in-plane load was to be 1500 lbs. using a design safety factor of 2.

An 8 inch box tube 42 inches long with $3/8$ inch thick walls was available and satisfied the design criteria. The anchor for the loading fixture was made from $1/2$ inch plate metal and bolted to the base structure as shown in Figures 2 and 3. A load cell was supported by a $1/2$ inch plate which was bolted to the anchor section.

The loading fixture, shown in Fig. 4, was machined from 4140 steel and was heat treated to a range of 38-42 on the Rockwell

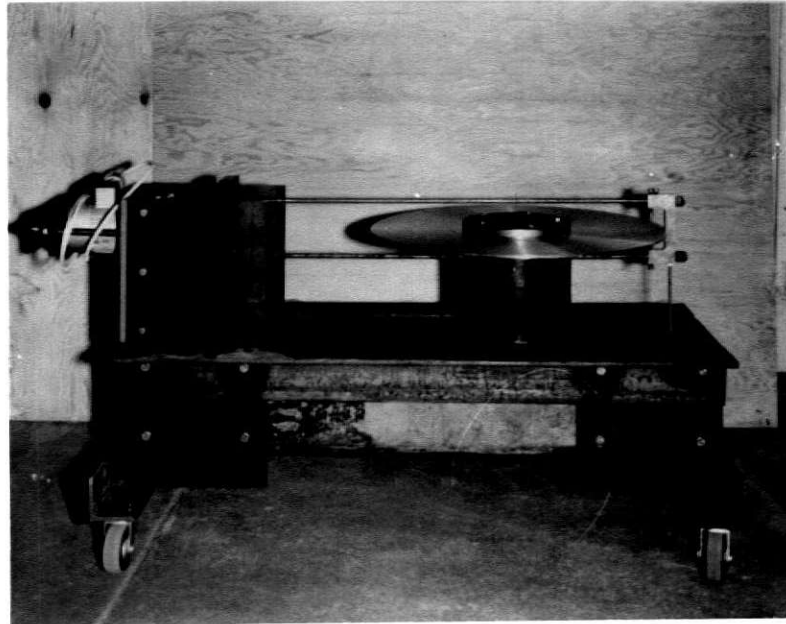


Figure 2

Photograph of the testing device.

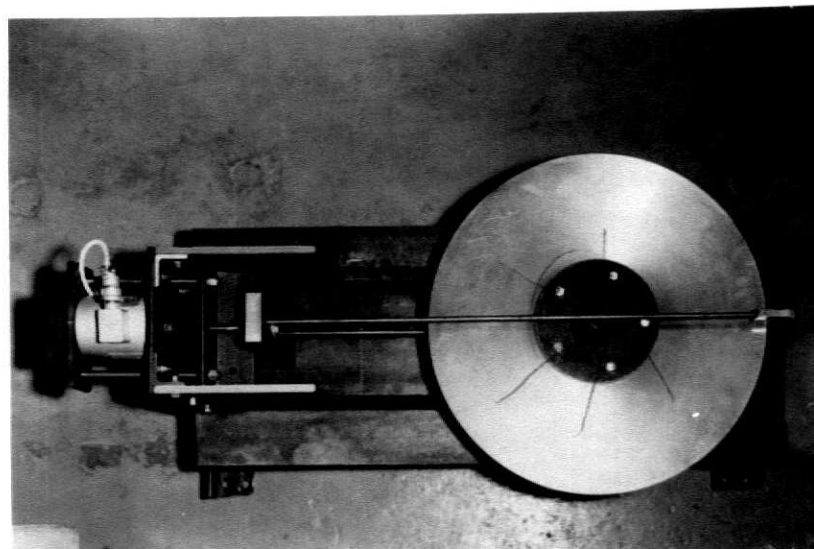


Figure 3

Photograph of the testing device.

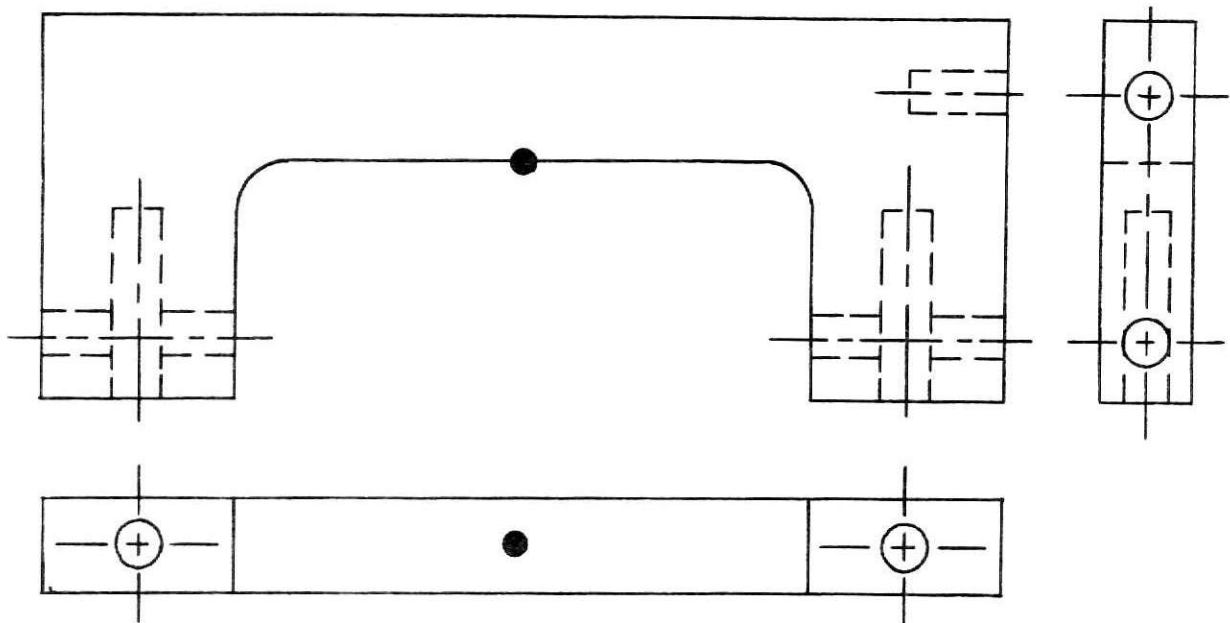


Figure 4

Three view full size loading fixture.

"C" hardness scale. The original load estimate was in error, as the critical load for the saw blade was 6300 lbs. This made it necessary to heat treat the loading fixture for additional strength. The hardness range gave the loading fixture a 7500 lb. maximum loading capability. A 1/8 inch spherical ball was pressed half-way into the center surface of the fixture to satisfy point 6 in the preliminary design criteria.

It was decided to use a long cable arrangement for applying the in-plane load to minimize the dampening of the transverse blade vibration. That consideration was to be for study of the problem without the pinned boundary condition at the load point. Two 1/8 inch stranded wire cables were used to connect the loading fixture and the nut and bolt load adjustment. The cables

were fastened to the loading fixture by set screws. This arrangement worked for a load range of 0-1500 lbs.

Upon redesign for larger loads, two 1/4 inch stranded wire cables were used. At approximately 2000 lbs. the cable began to slip. An alternate fastening arrangement was to drill the cable holes on through the loading fixture and weld or braze sleeves on the cable ends. Those ends began to break in a load range of 2500-3500 lbs. Time did not permit the use of engineered fittings by mail order. A decision was made to use 1/4 inch rod. The rods with welded sleeves were tested and found adequate up to 4000 lbs.

The critical load is in reference to a clamped-free blade. The critical load for the fixed point boundary condition would be higher than the clamped-free boundary but it was not calculated. However, it was only possible to load the blade to 3000 lbs. for testing.

The 1/8 inch ball was centered in the edge of the blade. As the load was applied the ball pressed into the blade causing permanent deformation. At approximately 3500 lbs. the inner surface of the loading fixture pressed against the blade edge which changes the boundary condition.

The clamping annulus was bolted to the cylinder with five bolts equally spaced around the annulus. The clamping annulus and the cylinder were turned on a lathe to a diameter of 7.875 inches. The annulus and the cylinder were marked for removing and replacing the annulus in the same position.

EXPERIMENTAL TECHNIQUE

The procedure for determining the frequencies of vibration, their mode shapes, and the variations with load had two parts. Part 1 was finding the resonant frequencies and their variations as the in-plane load varied. The second part was photographing the mode shape changes as the in-plane load varied. The reason for the two separate parts was the power requirement for resonance.

At resonance the phase angle between the excitation force and the transverse velocity of the blade was either 0° or 180° . The excitation force was input on the vertical axis and the velocity input on the horizontal axis of an oscilloscope. Resonance was detected when the Lissajous diagram changed to a slanted straight line on the cathode-ray tube (CRT).

Small forces were required to drive the blade at resonance. It was important to use minimum power in order to have a linear response in Part 1. It was important in Part 2 to obtain pure mode shapes by not over driving the blade.

The saw blade was excited by an electromagnetic shaker which was powered by a 200 watt power supply. A resistor was placed in the circuit in series between the shaker and the power supply. The voltage drop across the resistor was used as the excitation force input to the oscilloscope.

A velocity-meter and probe were used to input velocity to

the oscilloscope. The probe was small and its added mass and stiffness went undetected.

The driving probe and the velocity probe were placed in opposite regions of the blade where vibration occurred, as shown in Fig. 5. When the probes were on or close to nodal lines the amplitude of the Lissajous diagram at resonance was small.

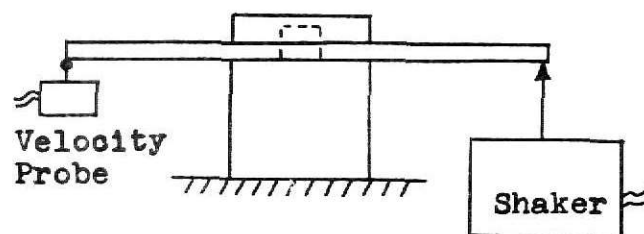


Figure 5

Shaker and velocity probe placement.

A digital counter was used to determine the frequency of the blade vibration by counting the output of the power supply. In Part 1 for the low power settings it was necessary to use a larger resistance in series with the power supply in order to trigger the counter which was voltage sensitive. The counter was equipped with a period counting circuit. By counting the period and inverting that number for the frequency more accuracy was obtained.

Graded Ottawa Fine sand was sprinkled on the blade and it bounced to positions where the acceleration was less than 32 ft/s^2 relative to the blade. Those patterns were photographed as an experimental description of the mode shapes for the resonant

conditions.

A 0-100,000 lb. compression load cell was used to measure the in-plane load. The load cell was calibrated in a 0-5000 lb. range. The strain indicator varied 20 micro strains per 500 lbs. The difference between two marks on the strain indicator was 5 micro strains and load increments were not taken less than 125 lbs. apart.

RESULTS

The blade dimensions and clamping geometry were input to a modification of Dubois (3) program which was done by Carlin (2). The experimental and theoretical results for the clamped free blade are shown in Fig. 6. It would be expected that the theoretical frequencies should be higher than the experimental frequencies for the corresponding number of nodal diameters. It should be noted again that the exact pre-stress condition of the blade was not known.

From the same modified program, frequency versus load data were tabulated in Table 1 and plotted in Figures 7-10. It was suspected that the one nodal diameter frequency response could be used as a comparison to the pinned point boundary condition. The relative amplitude of vibration at the point of load application was found to be several orders of magnitude smaller. That frequency response is shown in Fig. 8. From that graph in the 0-3000 lb. load range, the frequency only varies 0.3 Hz. Figures 11-15 are graphs of the experimental data for the first seven resonant conditions. For the pinned-point boundary condition, it is not possible to describe the modes in terms of nodal diameters and nodal circles. However, it was found that for certain frequencies the mode shapes did resemble the clamped-free blade since a nodal diameter was aligned with the load. The mode shapes in Figures 16, 19, 21, 25, 26, 27, and 28 are that type.

The data in Tables 2-6 are plotted in Figures 11-15, respectively. The third and fourth resonant conditions were not plotted since they were constant in the load range 0-3000 lbs.

Data for Run 1 were converted from period to frequency which accounts for the higher decimal place accuracy. That procedure was time consuming and did not prove to be a better approach in most cases. The counting interval for the frequency was 10 seconds. Data for Runs 2 and 3 were taken for a particular blade orientation. The difference was a rotation of 72 degrees from the data taken for Runs 2 and 3. It can be seen from the graphs that the 72 degree blade rotation gave the same results.

The experimental data shown in Fig. 12 did not compare to the theoretical data in Fig. 8. Figures 13 and 15 show a mode transition occurring in both cases at about 1500 lbs. The same situation seems to occur in Fig. 12 at 1500 lbs. This may partially explain the lack of correlation of Figures 8 and 12. The sand patterns for Figures 13 and 15 are Figures 21-22 and 25-28, respectively. The frequencies in Figures 21 and 22 are close and the different patterns might have caused the transition in the fifth resonant condition data.

The resonant condition patterns shown in Figures 17 and 18 were combinations of other mode shapes. However, the vibration at that frequency for the same power settings as all other patterns was the most violent. This resonant condition was not detected while taking the frequency load data. The pinned-point boundary condition made resonance sharp. In most cases the variation in mode shape was only to show a sharper sand pattern with

small variations in frequency.

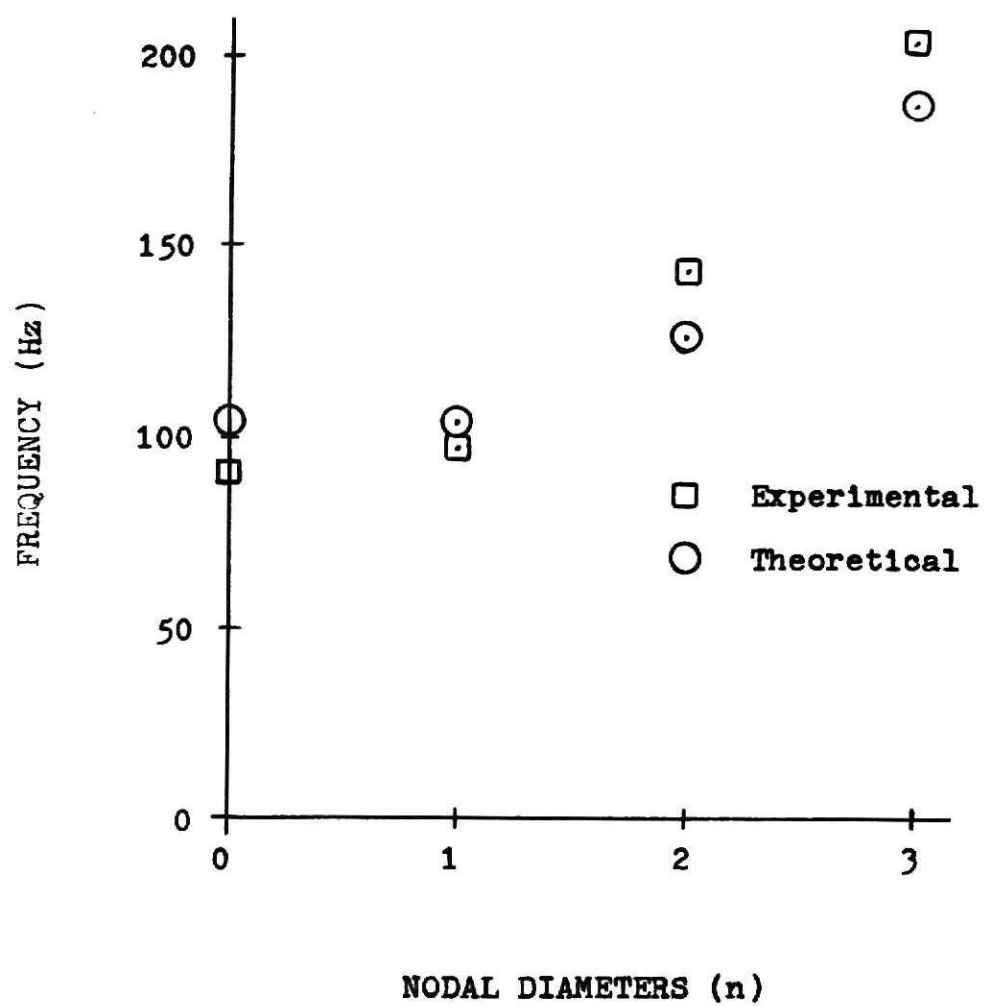


Figure 6

Frequency versus nodal diameters for the
clamped-free boundary.

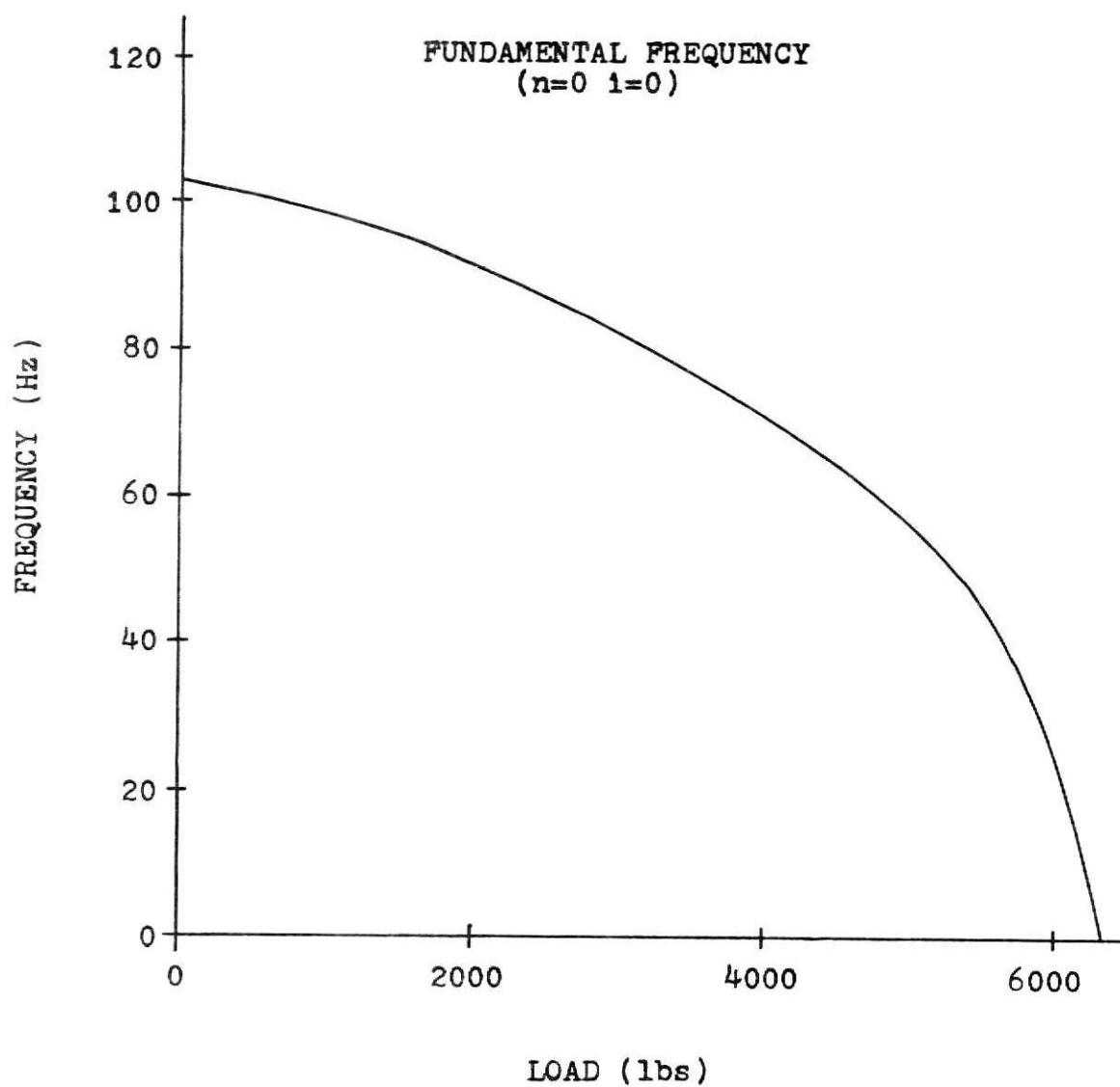


Figure 7

Theoretical frequency of a clamped-free
blade with radial in-plane load.

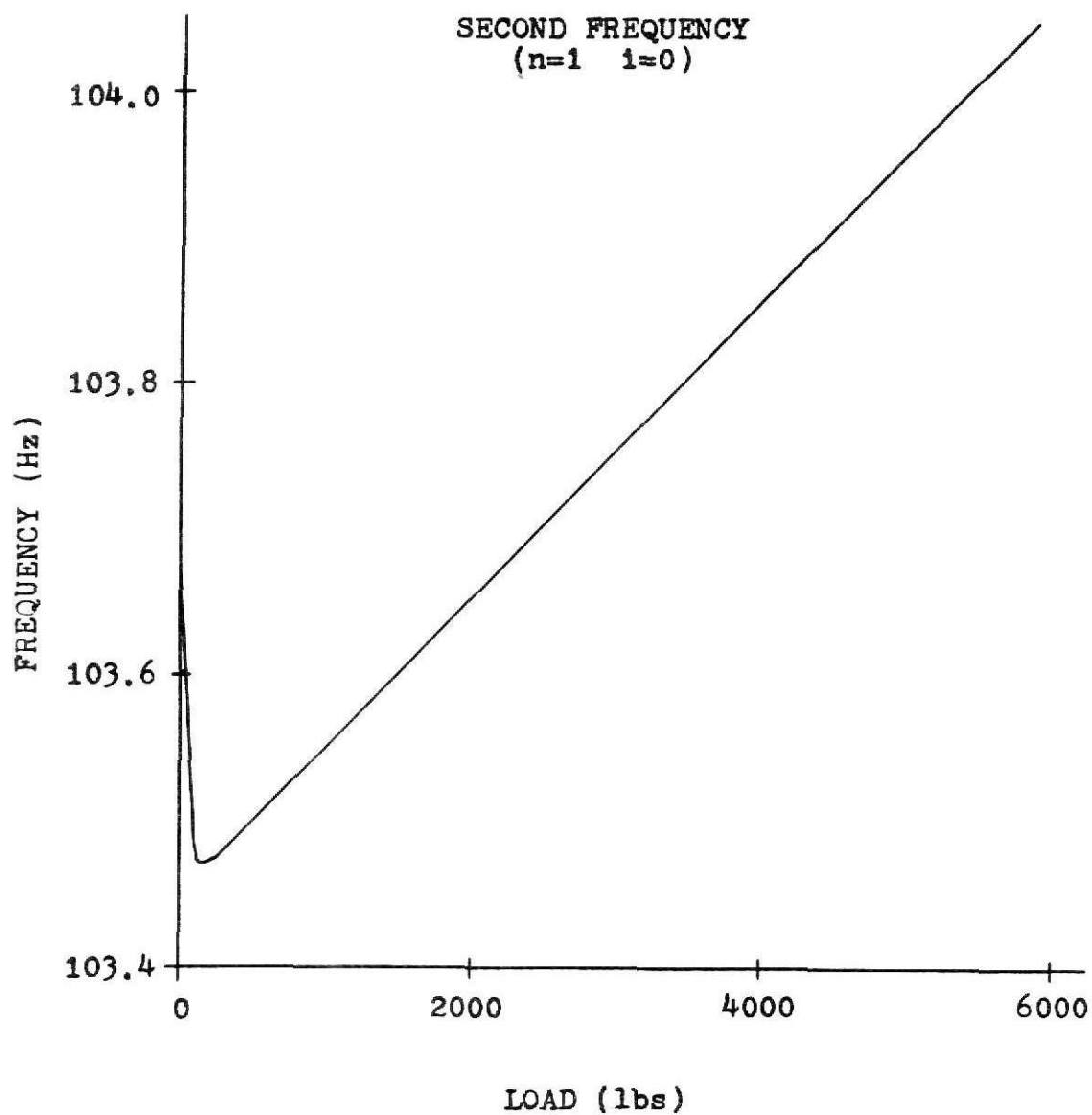


Figure 8

Theoretical frequency of a clamped-free blade
with radial in-plane load.

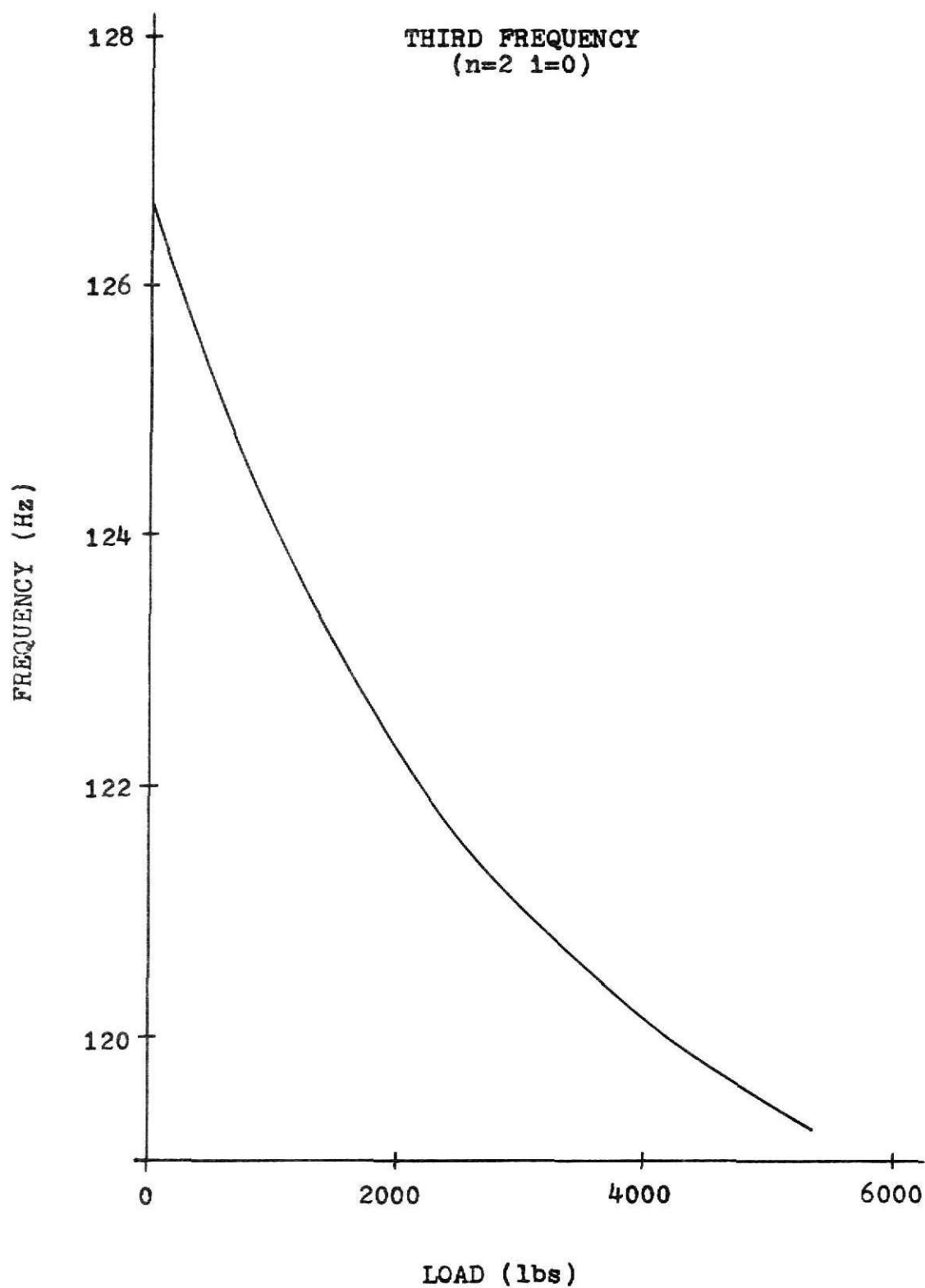


Figure 9

Theoretical frequency of a clamped-free blade
with radial in-plane load.

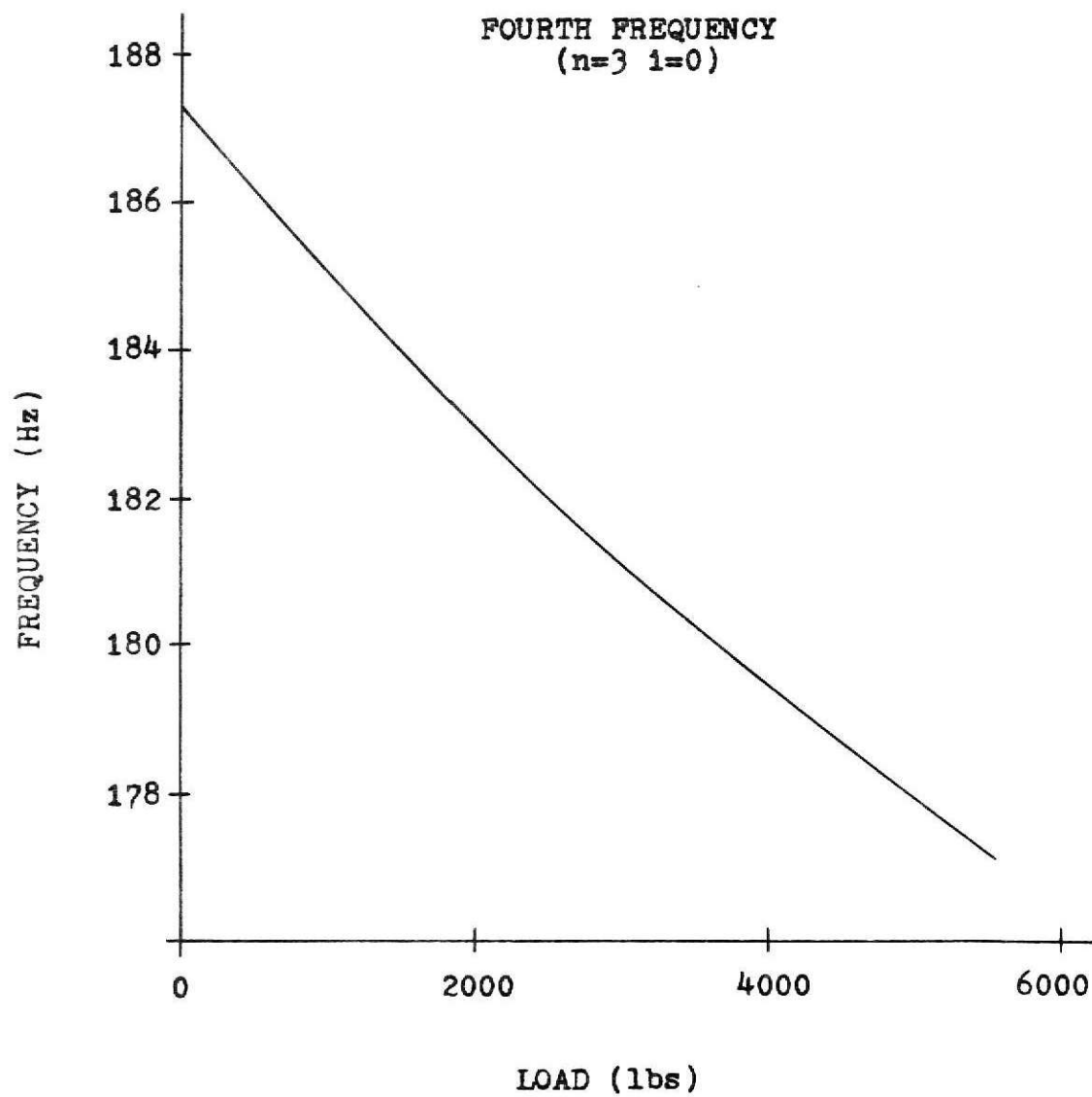


Figure 10

Theoretical frequency of a clamped-free blade
with radial in-plane load.

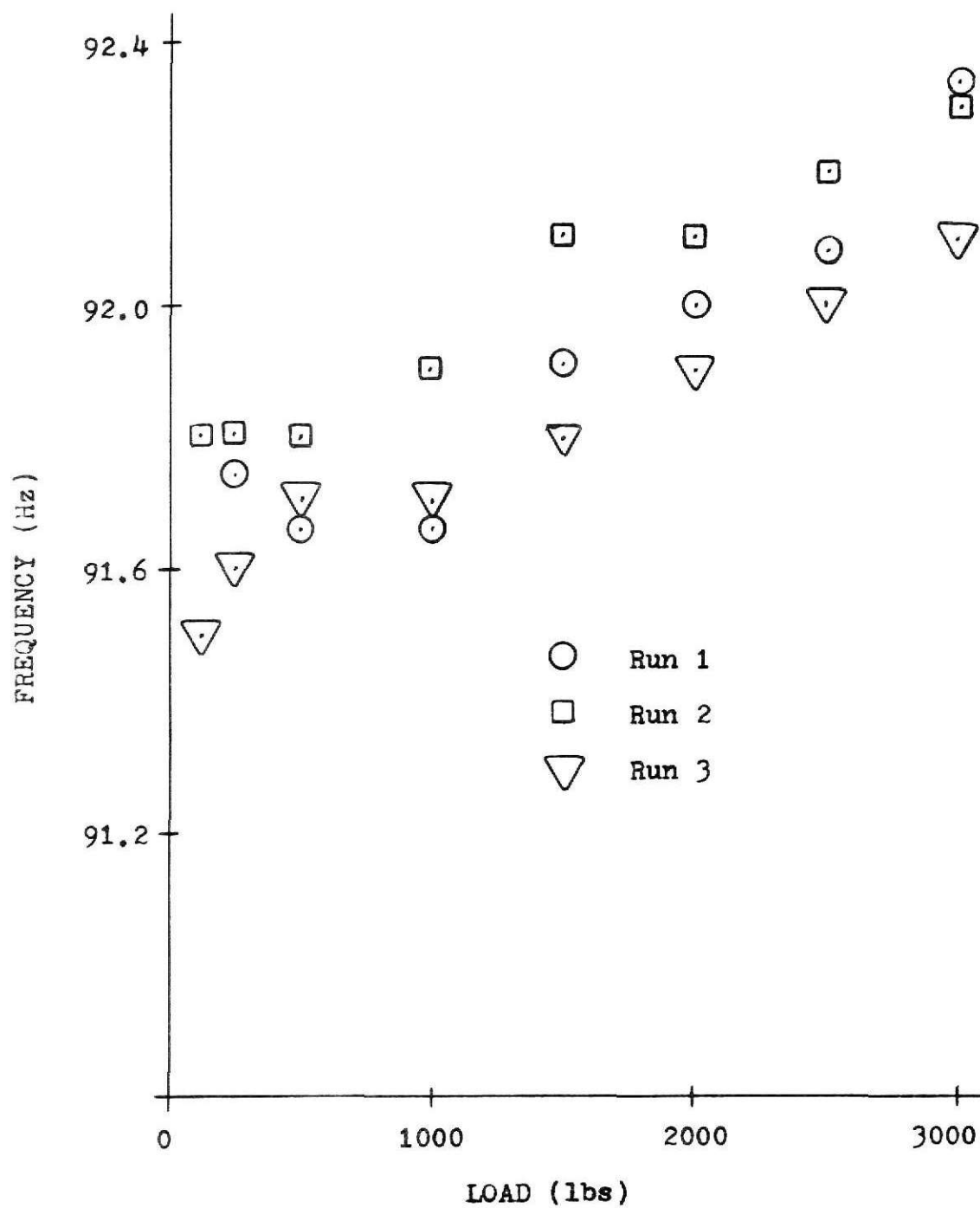


Figure 11

Frequency versus load for the
first resonant condition.

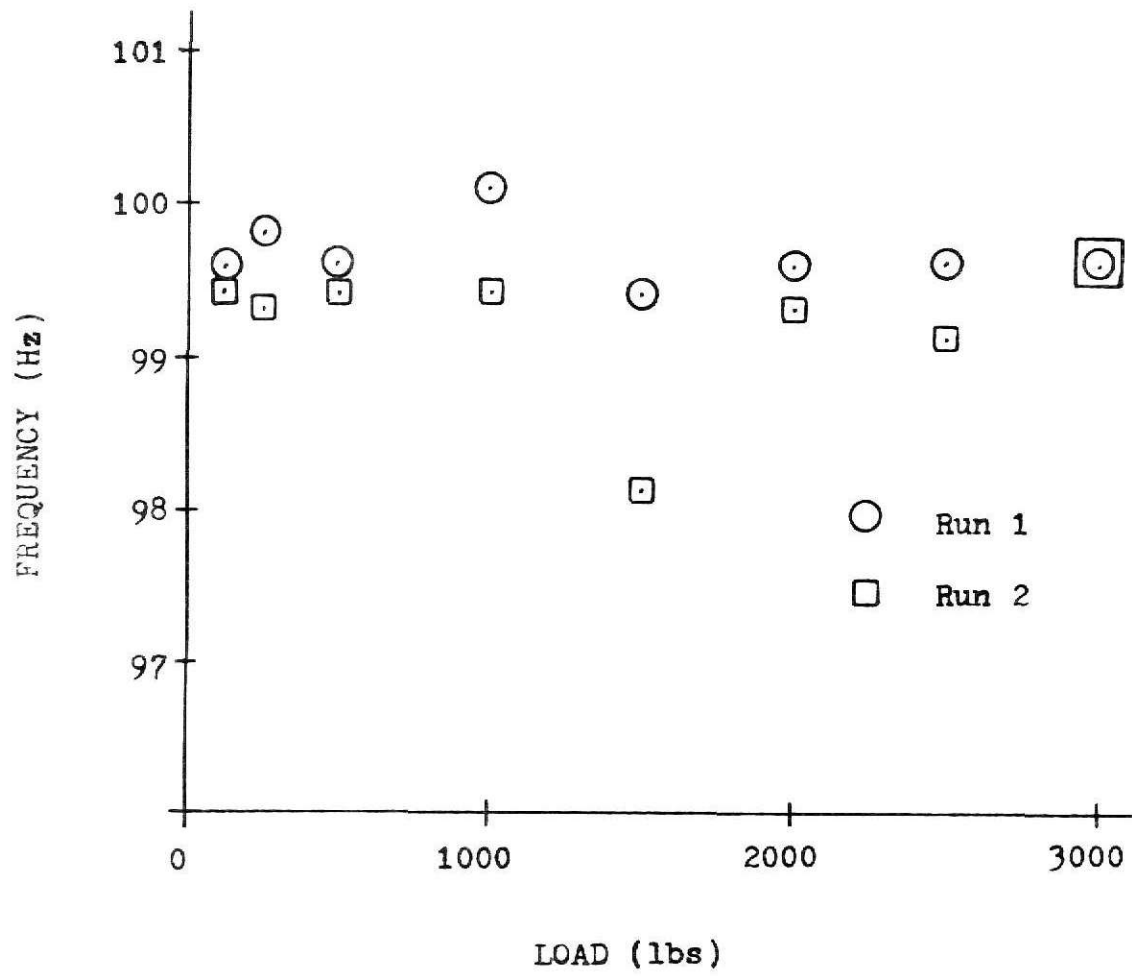


Figure 12
Frequency versus load for the second
resonant condition.

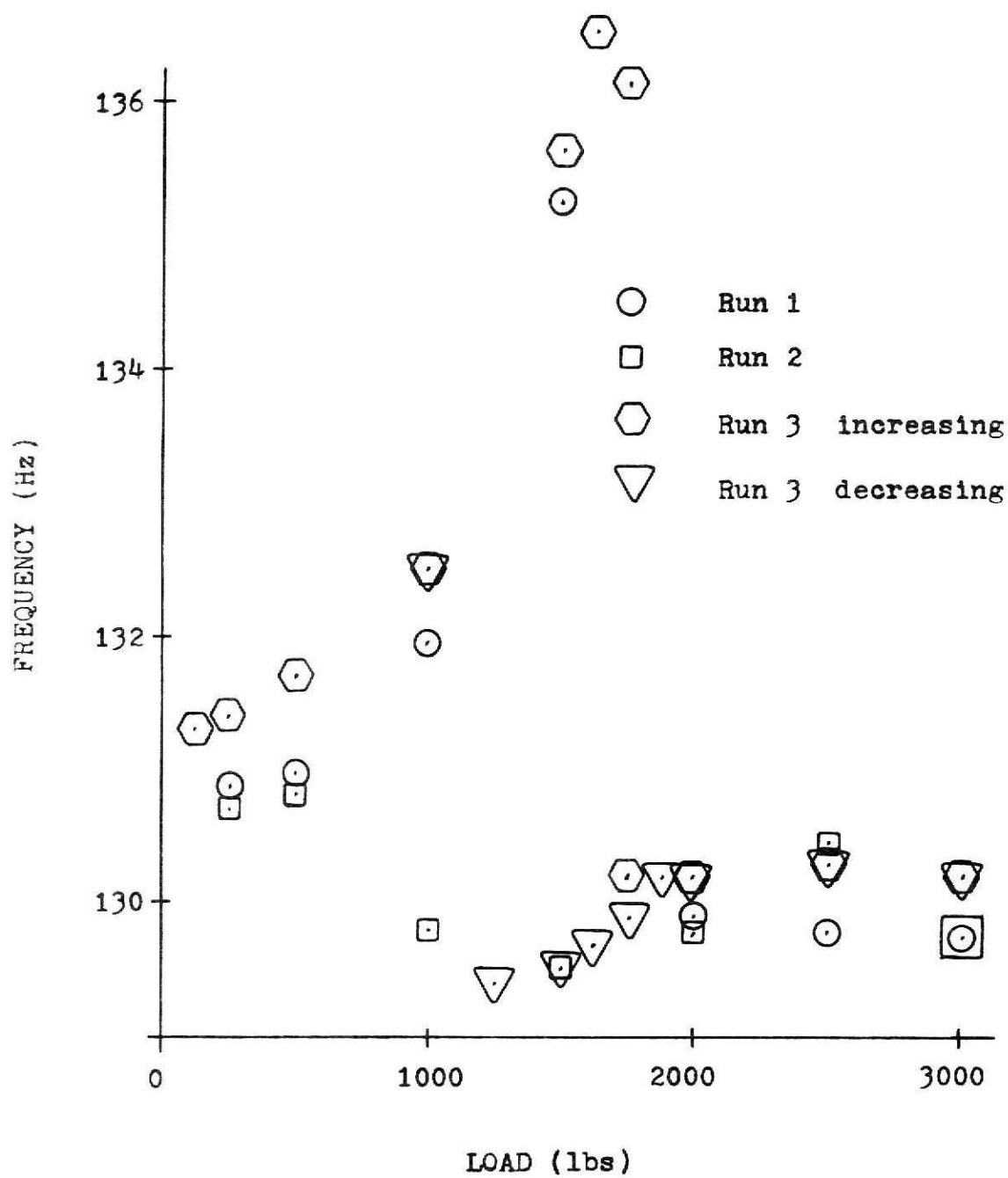


Figure 13

Frequency versus load for the fifth resonant condition.

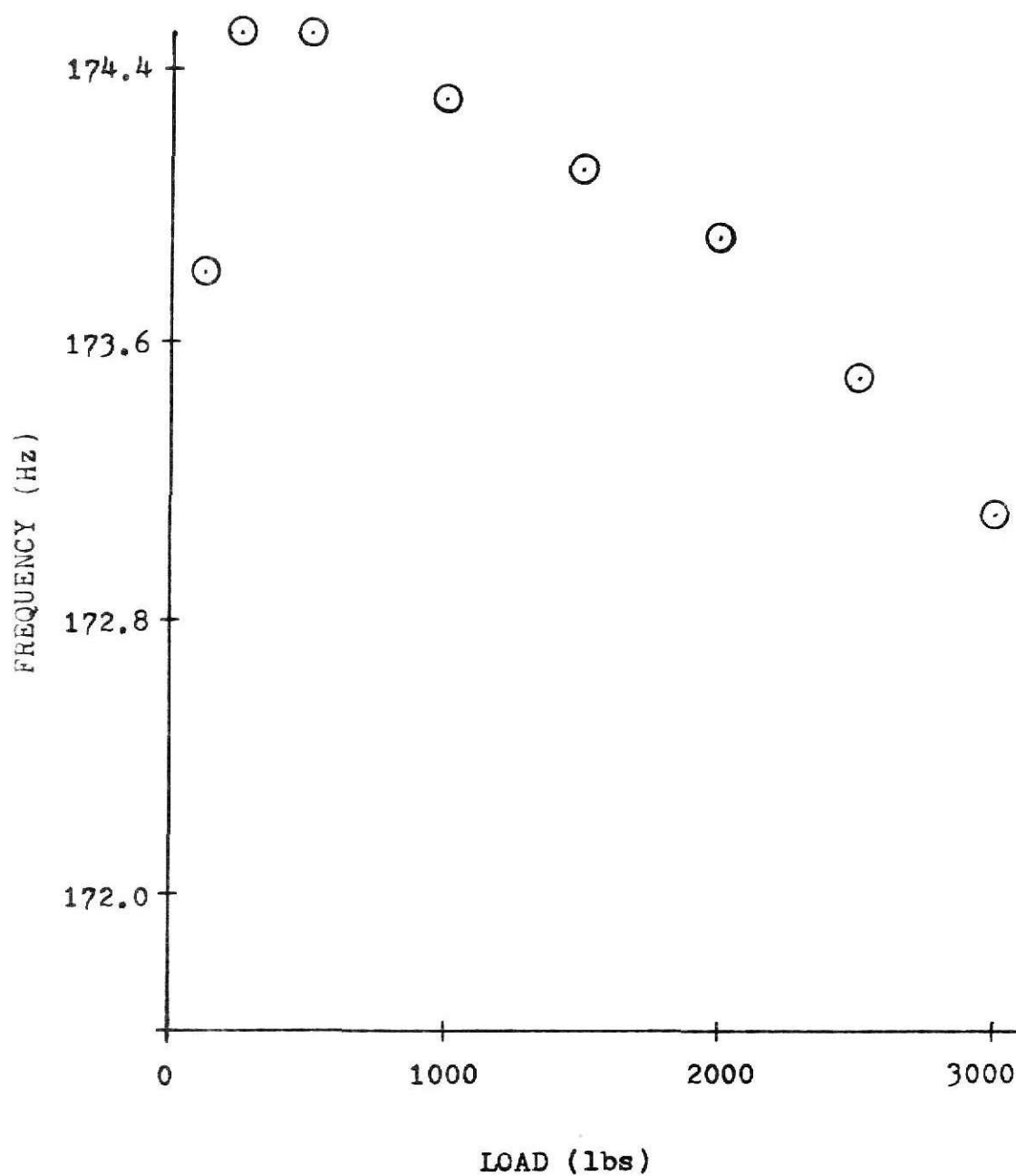


Figure 14

Frequency versus load for the sixth resonant condition.

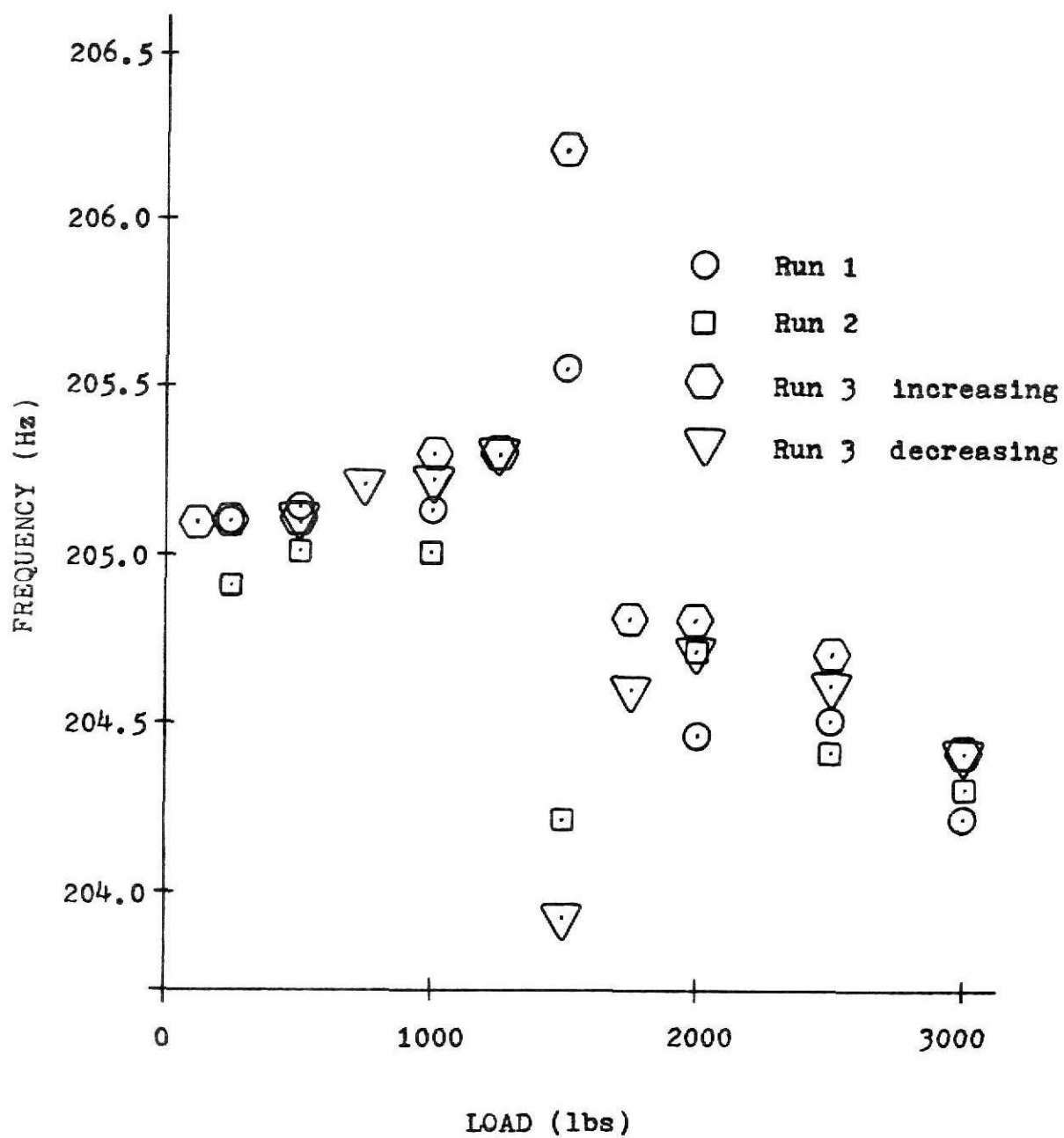
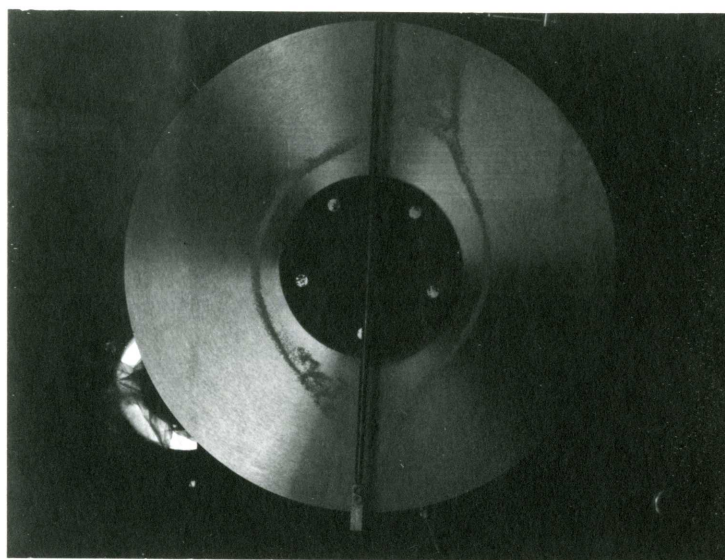


Figure 15

Frequency versus load for the seventh resonant condition.

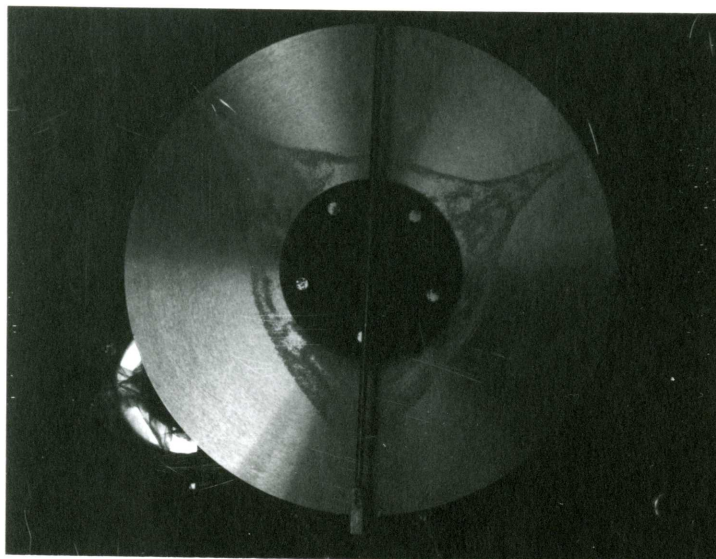


$F = 96 \text{ Hz}$

$P = 0-3000 \text{ lb.}$

Figure 16

Sand pattern for second
resonant condition mode shape.

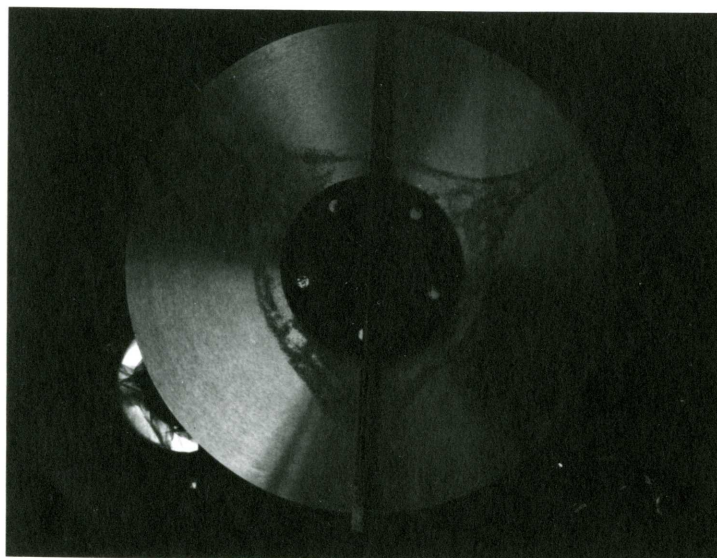


$F = 114 \text{ Hz}$

$P = 1000 \text{ lb.}$

Figure 17

Sand pattern mode shape
for a resonant condition.

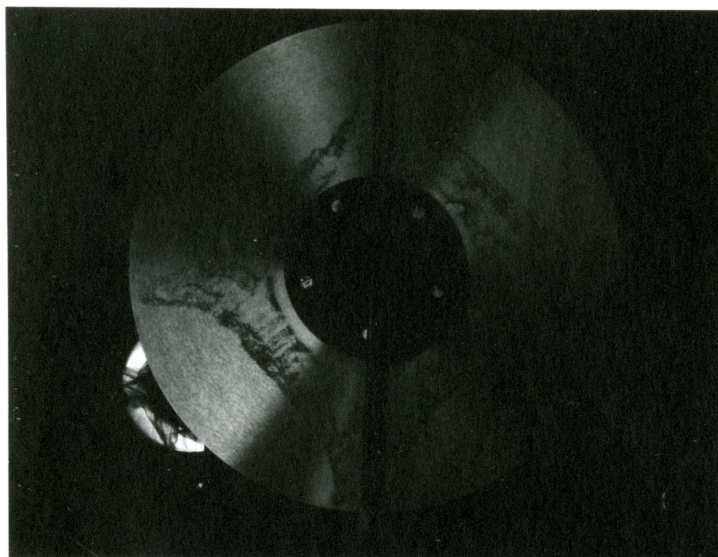


$F = 114 \text{ Hz}$

$P = 3000 \text{ lb.}$

Figure 18

Sand pattern mode shape
for a resonant condition.

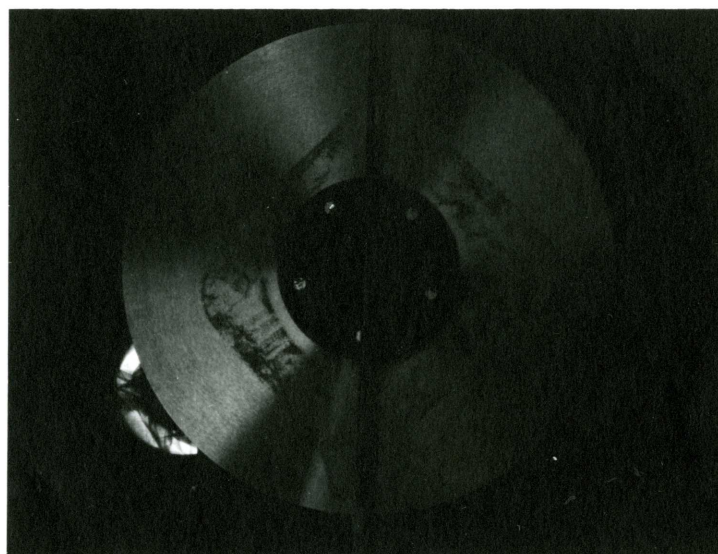


$F = 123 \text{ Hz}$

$P = 0-2000 \text{ lb.}$

Figure 19

Sand pattern mode shape for
the fourth resonant condition.

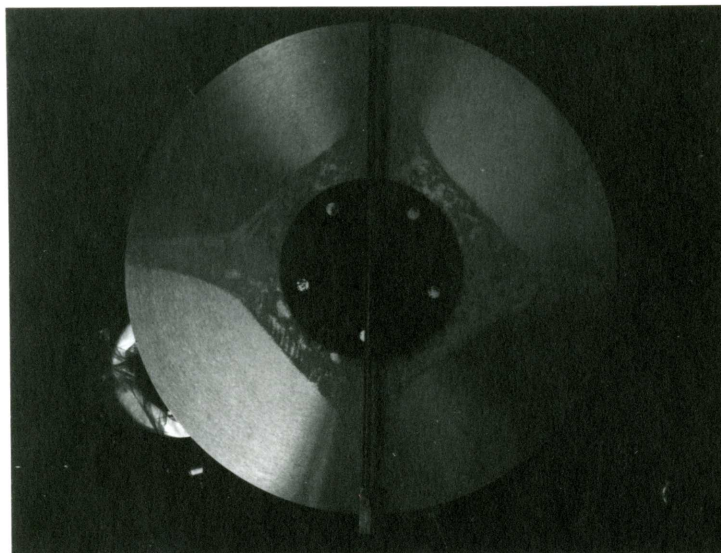


$F = 121 \text{ Hz}$

$P = 3000 \text{ lb.}$

Figure 20

Sand pattern mode shape for
the fourth resonant condition.

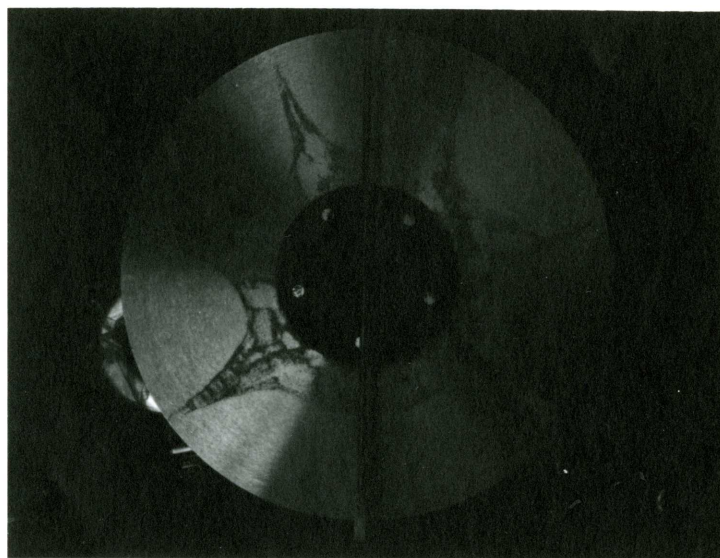


$F = 128 \text{ Hz}$

$P = 0-3000 \text{ lb.}$

Figure 21

Sand pattern mode shape for
the fifth resonant condition.

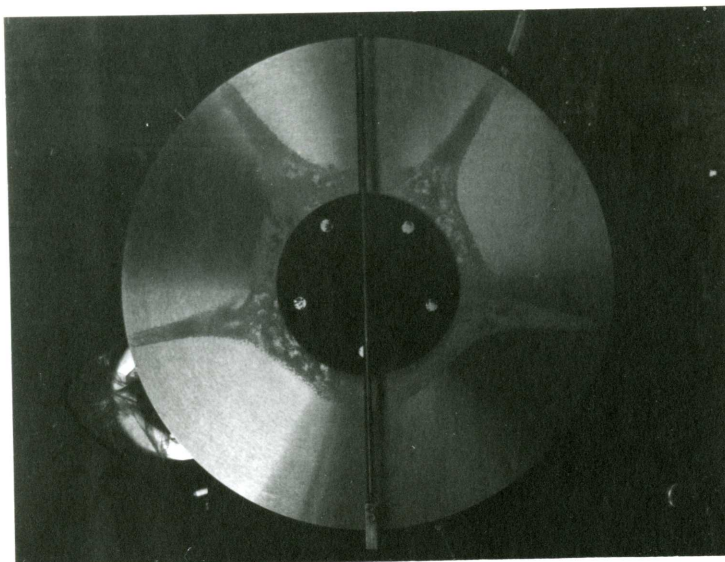


$F = 134 \text{ Hz}$

$P = 0-3000 \text{ lb.}$

Figure 22

Sand pattern mode shape
for a resonant condition.

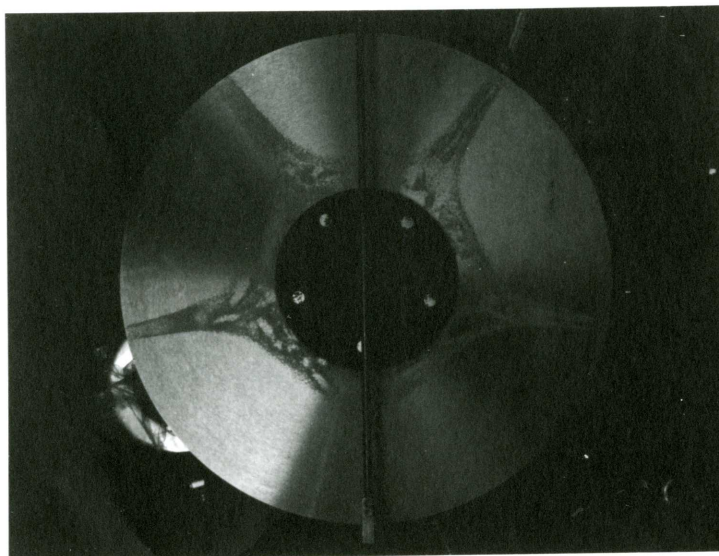


F = 173 Hz

P = 0-1500 lb.

Figure 23

Sand pattern mode shape for
the sixth resonant condition.

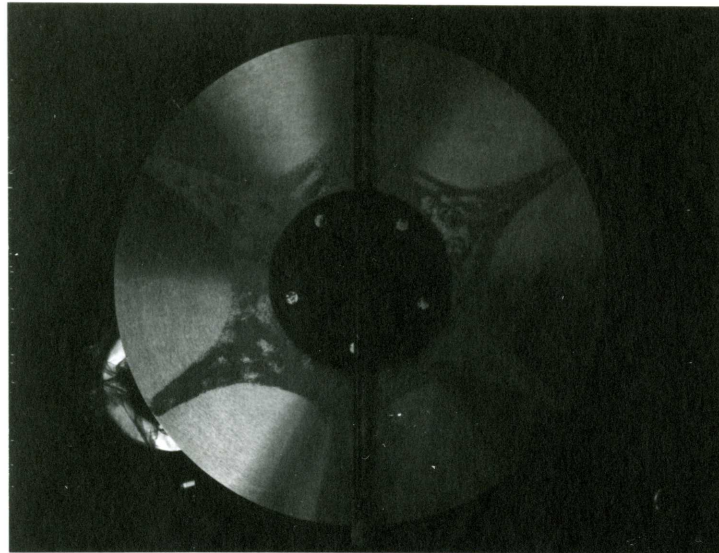


F = 172 Hz

P = 3000 lb.

Figure 24

Sand pattern mode shape for
the sixth resonant condition.

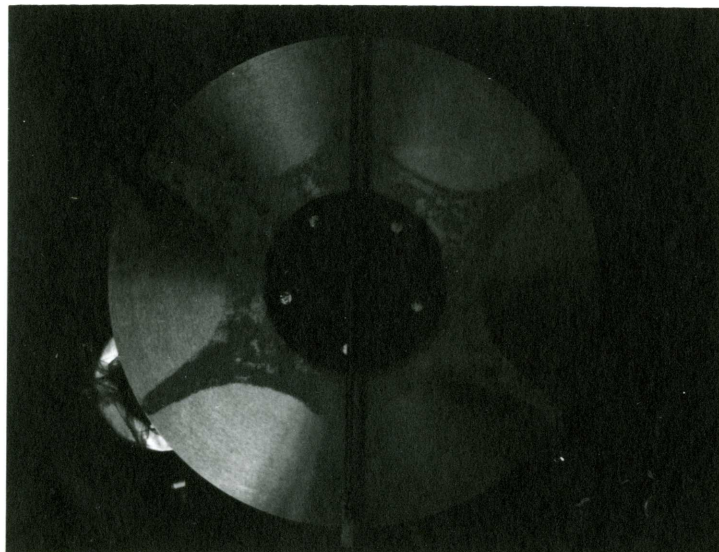


$F = 203 \text{ Hz}$

$P = 1000 \text{ lb.}$

Figure 25

Sand pattern mode shape for
the seventh resonant condition.

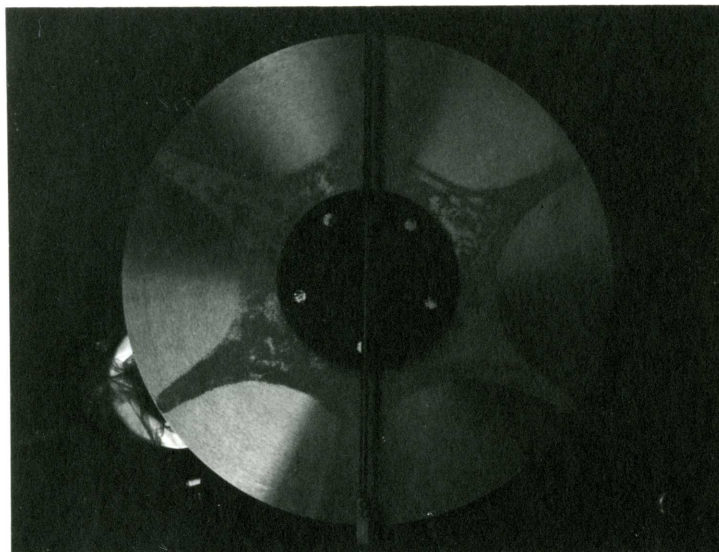


$F = 203 \text{ Hz}$

$P = 1500 \text{ lb.}$

Figure 26

Sand pattern mode shape for
the seventh resonant condition.

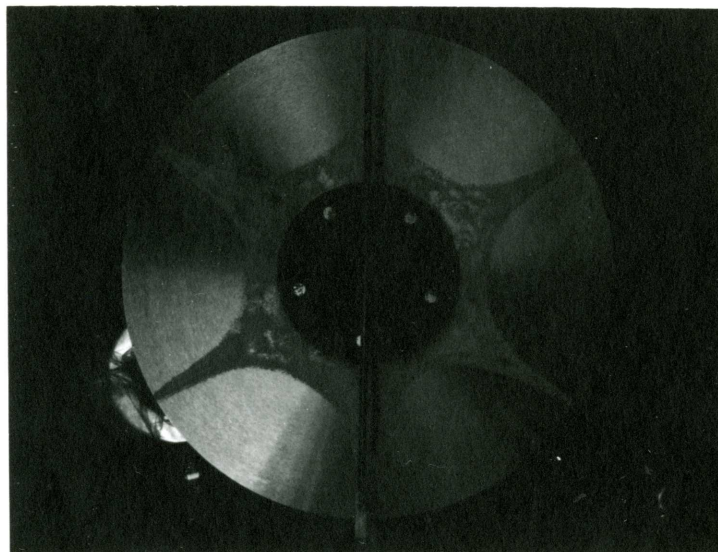


$F = 203 \text{ Hz}$

$P = 2000 \text{ lb.}$

Figure 27

Sand pattern mode shape for
the seventh resonant condition.



$F = 203 \text{ Hz}$

$P = 3000 \text{ lb.}$

Figure 28

Sand pattern mode shape for
the seventh resonant condition.

CONCLUSIONS

An experimental determination of the frequency variation with changing in-plane concentrated radial loads to buckling was not achieved. Since the loading fixture pressed into the blade edge, only in-plane loads from 0-3000 lbs. were applied and those frequency changes recorded. The frequency change in all resonant conditions was small. The unexpected small frequency variation might have been larger if the load had approached the buckling load.

The sand patterns were sharper with increasing load. The pinned-point boundary condition made resonance and the sand patterns sharper.

The test jig could be used in the future to determine the effect of tensioning on the buckling load. If a further study were to be conducted, the problem should be scaled down by testing thinner blades which would reduce the critical load to less than 3000 lbs. The more fundamental problem, the clamped-free boundary condition, could be studied if a method were devised to vibrate the blade without coupling the mass of the loading fixture to the vibrating system. One approach might be to vibrate the load with a fixed displacement thus vibrating the blade as an isolated system.

SELECTED BIBLIOGRAPHY

- (1) Bryan, G. H. "On the Stability of a Plane Plate Under Thrusts in its Own Plane, With Applications to the 'Buckling' of the Sides of a Ship." Proc. London Math. Soc., 22:54-67, 1891.
- (2) Carlin, J. F. "The Effects of Tensioning on The Buckling and Vibration of Circular Saw Blades." (unpub. Master's Report, Kansas State University, 1971.)
- (3) DuBois, R. P. "Buckling Loads of Tensioned Circular Plates Subject to Concentrated In-Plane Loading." (unpub. Master's Report, Kansas State University, 1970.)
- (4) Holman, J. P. Experimental Methods for Engineers. New York: McGraw-Hill, Inc., 1966.
- (5) Kirchhoff, G. "Ueber die Schwingungen einer Elastischen Scheibe." Crelle's Journal, 40:51-88, 1850.
- (6) Southwell, R. V. "On the Free Transverse Vibrations of a Uniform Circular Disc Clamped at its Center; and on the Effects of Rotation." Proc. Royal Soc. of London, Series A, 101:133-153, 1922.
- (7) St. Cyr, W. W., II. "Vibration and Stability of Circular Plates Subjected to Concentrated In-Plane Forces." (unpub. Ph.D. dissertation, Kansas State University, 1965.)

APPENDIX

The following tables and graphs contain theoretical and experimental load-frequency data.

TABLE 1
THEORETICAL LOAD FREQUENCY DATA FOR THE
CLAMPED-FREE SAW BLADE

De = 21.625 in. Per = 6311.11 lb. h = .1545 in.
Db = 7.875 in. Da = 3.00 in.

P	n=0 i=0 (Hz)	n=1 i=0 (Hz)	n=2 i=0 (Hz)	n=3 i=0 (Hz)	n=0 i=1 (Hz)
0.00	103.30	103.64	126.39	187.29	667.77
788.89	99.67	103.51	124.46	185.49	666.14
1577.78	94.66	103.61	122.93	183.82	663.91
2366.66	88.35	103.71	121.75	182.27	660.95
3155.55	80.59	103.81	120.86	180.83	657.21
3944.44	71.02	103.91	120.19	179.50	652.72
4733.33	58.92	104.01	119.67	178.27	647.55
5522.22	42.28	104.11	119.26	177.12	641.81

TABLE 2
EXPERIMENTAL LOAD FREQUENCY DATA
FOR THE FIRST RESONANT CONDITION

	P (lb)	Run 1 (Hz)	Run 2 (Hz)	Run 3 (Hz)
	125	*****	91.8	91.5
	250	91.74	91.8	91.6
	500	91.66	91.8	91.7
R = 10.812 in.	1000	91.66	91.9	91.7
Rb = 2.937 in.	1500	91.91	92.1	91.8
Ra = 1.500 in.	2000	92.00	92.1	91.9
h = .1545 in.	2500	92.08	92.2	92.0
	3000	92.34	92.3	92.1

TABLE 3
EXPERIMENTAL LOAD FREQUENCY DATA
FOR THE SECOND RESONANT CONDITION

	P (lb)	Run 1 (Hz)	Run 2 (Hz)
	125	99.60	99.4
	250	99.80	99.3
R = 10.812 in.	500	99.60	99.4
R _b = 2.937 in.	1000	100.10	99.4
R _a = 1.500 in.	1500	99.40	98.1
h = .1545 in.	2000	99.60	99.3
	2500	99.60	99.1
	3000	99.60	99.6

TABLE 4
EXPERIMENTAL LOAD FREQUENCY DATA
FOR THE THIRD, FOURTH, AND SIXTH
RESONANT CONDITIONS

	P (lb)	THIRD (Hz)	FOURTH (Hz)	SIXTH (Hz)
	125	100.5	120.0	173.8
	250	100.5	120.0	174.5
R = 10.812 in.	500	100.5	120.0	174.5
R _b = 2.937 in.	1000	100.5	120.0	174.3
R _a = 1.500 in.	1500	100.5	120.0	174.1
h = .1545 in.	2000	100.5	120.0	173.9
	2500	100.5	120.0	173.5
	3000	100.5	120.0	173.1

TABLE 5
EXPERIMENTAL LOAD FREQUENCY DATA
FOR THE FIFTH RESONANT CONDITION

	P (lb)	Run 1 (Hz)	Run 2 (Hz)	Run 3 (Hz)
	125	*****	*****	131.3
	250	130.87	130.7	131.4
	500	130.96	130.8	131.7
	1000	131.94	129.8	132.5
	1500	135.23	129.5	135.6
	2000	129.80	129.8	130.2
	2500	129.77	130.4	130.3
	3000	129.74	129.7	130.2
R = 10.812 in.				
R _b = 2.937 in.				
R _a = 1.500 in.	1625	Run 3 load increasing		136.5
h = .1545 in.	1700			136.2
	1750			130.2
	1875	Run 3 load decreasing		130.2
	1750			129.9
	1625			129.7
	1500			129.5
	1250			129.4
	1000			132.5

TABLE 6
EXPERIMENTAL LOAD FREQUENCY DATA
FOR THE SEVENTH RESONANT CONDITION

	P (lb)	Run 1 (Hz)	Run 2 (Hz)	Run 3 (Hz)
	125	*****	*****	205.1
	250	205.09	204.9	205.1
	500	205.13	205.0	205.1
	1000	205.13	205.0	205.3
	1250	*****	*****	205.3
	1500	205.55	204.2	206.2
	1750	*****	*****	204.8
	2000	204.46	204.7	204.8
	2500	204.50	204.4	204.6
	3000	204.21	204.3	204.4
	2500	Run 3 load decreasing		204.6
	2000			204.7
	1750			204.6
	1500			203.8
	1250			205.3
	1000			205.2
	750			205.2
	500			205.1
	1000	Run 3 load increasing		205.3
	1500			206.2
	1750			204.8
	2000			204.8
	2500			204.6
	3000			204.4

$R = 10.812$ in.
 $R_b = 2.937$ in.
 $R_a = 1.500$ in.
 $h = .1545$ in.

ACKNOWLEDGEMENTS

I would like to express my appreciation for the efforts of Dr. F.C. Appl with the report and Dr. H.S. Walker in the laboratory. I would like to thank Jerry Carlin for his assistance, also.

VITA

Ronald R. Leathers

Candidate for the Degree of

Master of Science

Report: THE EFFECTS OF IN-PLANE RADIAL LOADS ON THE VIBRATION
OF CIRCULAR SAW BLADES

Major Field: Mechanical Engineering

Biographical:

Personal Data: Born in Dodge City, Kansas, December 15,
1945, the son of Roy R. and Louise F. Leathers.

Education: Graduated from Satanta Rural High School in May,
1963; received the Bachelor of Science degree in June,
1969; completed requirements for the Master of Science
degree in July, 1971.

Professional experience: Worked as an Associate Engineer
for the Boeing Company from June, 1969, to June, 1971.

THE EFFECTS OF IN-PLANE RADIAL LOADS
ON THE VIBRATION OF CIRCULAR
SAW BLADES

by

RONALD R. LEATHERS

B.S., Kansas State University, 1969

AN ABSTRACT OF A MASTER'S REPORT

submitted in partial fulfillment of the

requirements for the degree

MASTER OF SCIENCE

Department of Mechanical Engineering

KANSAS STATE UNIVERSITY
Manhattan, Kansas

1971

ABSTRACT

A number of studies has shown that the buckling load can be altered significantly for constant-thickness, centrally clamped, circular disks. The idea that circular saw blades may be loaded to buckling during normal operating conditions has created particular attention. The variation of natural frequencies with varying in-plane concentrated, radial loads is experimentally examined here for a stationary, constant-thickness, centrally clamped, circular saw blade with a pinned-point boundary at the point of load application.

A loading device and testing fixture were designed. A linear frequency response (meaning the lateral amplitude was very small compared to the blade thickness) with varying load was determined for a maximum load of approximately one-half the critical load for a clamped-free blade. The mode shapes of vibration were photographed for varying loads.

For the load range investigated the frequency variation was small. The pinned-point boundary condition made resonance and the sand patterns sharper. It was found that the pinned-point boundary condition made the discussion of mode shapes in terms of nodal circles and nodal diameters difficult.